

Article - Human and Animal Health

# A Novel Clip Limit Estimation Technique for Blood Vessel Segmentation and OD/OS Classification Technique for Retina Images

**Vijaya Maheswari MuthuKumara Samy**<sup>1\*</sup>  
https://orcid.org/0000-0002-8556-5996

**Muthulakshmi Murugaiah**<sup>4</sup>  
https://orcid.org/0000-0003-1833-5311

**Murugeswari Ganesan**<sup>2</sup>  
https://orcid.org/0000-0002-7356-518X

**Jency Rajakumari Jeyabose Thanaraj**<sup>5</sup>  
https://orcid.org/0000-0003-1292-9872

**Aravind Kumar Karunakaran**<sup>3</sup>  
https://orcid.org/0000-0003-4966-4679

<sup>1</sup>Manonmaniam Sundaranar University, Department of Computer Science and Engineering, Tirunelveli, Tamil Nadu, India; <sup>2</sup>Manonmaniam Sundaranar University, Department of Computer Science and Engineering, Tirunelveli, Tamil Nadu, India; <sup>3</sup>Manonmaniam Sundaranar University, Department of Computer Science and Engineering, Tirunelveli, Tamil Nadu, India; <sup>4</sup>Kalasalingam Academy of Research and Education, Department of Computer Science and Engineering, Srivilliputhur, Tamil Nadu, India; <sup>5</sup>Manonmaniam Sundaranar University, Department of Computer Science and Engineering, Tirunelveli, Tamil Nadu, India.

Editor-in-Chief: Paulo Vitor Farago  
Associate Editor: Paulo Vitor Farago

Received: 21-Oct-2022; Accepted: 31-May-2023

\*Correspondence: vinusankar0306@gmail.com; Tel.: +91-8870300190 (V.M.M.S.)

## HIGHLIGHTS

- Technique for identification of OD/OS using DWT is proposed.
- Clip limit estimation using different analytical strategies is proposed.
- A framework for blood vessel extraction is presented.
- The proposed techniques are tested on DRIVE, HRF, STARE, DIARETDB1 and VAMPIRE datasets.
- The proposed technique is compared with existing techniques.

**Abstract:** The evolution of digital health care system in medical imaging has become a contemporary area. Human eye contain numerous nerves and sensitive tissues in it which are highly prone to eye diseases like hemorrhage, exudates, micro aneurysms etc. These eye diseases may affect blood vessels of retina to a greater extent. There are different research contributions made in this research work. They are (i) Identification of OD/OS (Right eye / Left eye) using DWT. (ii) A clip limit estimation technique which identifies the suitable clip limit value for enhancement. (iii) A framework for blood vessel extraction using estimated clip limit value and thresholding technique. Using DWT the localization of optic disc is done. The clip limit estimation technique involves various analysis to estimate the suitable clip limit for enhancement namely qualitative analysis, quantitative analysis, intensity distribution analysis and statistical analysis. A framework is proposed for retina blood vessel segmentation using clip limit estimation technique. The performance of

the proposed methods are measured in terms of classification accuracy, sensitivity, specificity. The framework is tested on different datasets which produced an accuracy of 96.87% on DRIVE dataset, 96.89% on HRF dataset, 97.34% on STARE dataset, and 97.52% on DIARETDB1 dataset respectively.

**Keywords:** Oculus Sinister (OS); Oculus Dexter (OD); Clip Limit; Clipping Process; Blood vessels; Retina.

---

## INTRODUCTION

The human eye is a sense organ that receives light signals and transfers it to the brain – fundamentally, it reacts to light energy and converts it into vision. The eye is made up of constituent parts that include the cornea, pupil, iris, optic nerve, lens, macula, choroid, conjunctiva, retina and the vitreous. Eye diseases can be due to the metabolic disorder of the retina [1]. The retina is a thin nervous tissue that covers the human eye. Retinal nerves, which are connected to the brain, convert a light signal into a neural signal prior to transferring it to the brain. The central retinal artery plays a critical role in supplying blood to all parts of the retina, bifurcating into branches of blood vessels. These blood vessels have a specific role to play in that they carry blood and oxygen to all parts of the retina. Made up of the thinnest tissue, the retina is greatly disease-prone [2]. With the relentless onset of online technology the world over, the near-constant use of electronic gadgets by adolescents has put their vision at risk, particularly in terms of damage to the optic disc and retinal blood vessels. Retinal disorders include hemorrhages, retinal detachment, diabetic retinopathy, micro aneurysms, hard exudates and soft exudates. People who suffer from an eye disorder must, of necessity, have their eyes examined every year to ascertain its severity. Treatment is based on the extent of retinal damage. In certain cases, however, eye disorders cannot be treated. Retinal cells, for instance, which die when there is little or no blood supply cannot be restored. While untreated eye disorders may culminate in blindness, early detection helps avert the risk of vision loss. Damage to retinal arteries or veins causes cardiovascular problems and stroke, apart from a very real threat of eye disorders. Ophthalmologists routinely examine damage to retinal blood vessels to determine the incidence of retinal eye disease. The earlier the diagnosis is provided, the better can monitor and control the consequences of the disease [3]. Like the blood vessels, the optic disc plays a key role in transferring visual information to the brain. The optic disc, or optic nerve head, is located at the back of the eye. The opening or entry point of the blood vessels in the eye commences with the optic disc supplying blood to all parts of the retina. In general, the optic disc is orange. A pale color is indicative of abnormalities like glaucoma, inflammation, pain in the eyes and loss of peripheral vision or double vision, among others. Depending on the damage to the optic disc, disease severity may range from distorted vision to blindness. The brain cannot receive visual information with a defective optic disc. Given that the entry point of the blood vessels commences at the optic disc, there is every chance of hemorrhage, inflammation, or the presence of micro aneurysms where diabetic patients are concerned. Image processing techniques play a principal role in identifying retinal diseases. A range of image processing techniques like edge detection and segmentation are used to extract blood vessels, following which deformities like micro aneurysms, hard exudates and soft exudates are identified.

This work proposes the two techniques below for retinal image analysis:

- i. Identifying the Oculus Dexter (OD) or right eye and Oculus Sinister (OS) or left eye using the DWT,
- ii. Extracting retinal blood vessels using a clip limit estimation technique.

A retinal image analysis in medical imaging is crucial to detecting retinal abnormalities. Sizable contributions have been made in this direction by researchers, particularly in terms of optic disc region estimation and retinal blood vessel extraction. Ozkava and coauthors [4] used adaptive thresholding with a Gaussian Window to estimate vessel geometry and a Wiener filter to de-noise the image. Aswini and coauthors [5] proposed a technique that used top-hat transformation for smoothing and a two-fold hysteresis algorithm for blood vessel extraction. Ganesan and Sathish [6] used a technique that incorporated the Ipachi model to measure blood vessel boundaries. Image intensity details and a local phase-based enhancement technique are combined to preserve the characteristics of the vessels. Dash and coauthors [7] developed a technique that uses a 2D Gabor wavelet and geodesic operators to extract blood vessels. Ramos-Soto and coauthors [8] used a two-step technique for the same. In step 1, thick blood vessels are extracted using homomorphic and median filtering. In step 2, thin vessels are extracted using the MCET-HHO multilevel algorithm. Xue and coauthors [9] proposed a technique which uses optimal thresholding and gray histogram thresholding, while Lestari and coauthors [10] used a Gaussian filter. Rahmani and coauthors [11] used an unsharp filter to sharpen blood vessels, followed by an optimal Gabor filter and morphological

reconstruction for their extraction. The Kohonen clustering method is applied to the preprocessed image to differentiate between retinal vessels and non-vessels. Nugroho and coauthors [12] used a 2D Gabor wavelet along with morphological reconstruction, while Yavuz and coauthors [13] used the top-hat transform and a Gabor filter to enhance the vessels, following which p-tile thresholding is applied for extraction. Sathya and coauthors [14] used a multi-scale contourlet transform on the contrast- enhanced image to the same end. Halder and coauthors [15] used the CLAHE for contrast enhancement. A median filter is applied on the image, along with morphological operations for blood vessel extraction. Dash and coauthors [16] used the CLAHE for contrast enhancement, along with morphological filtering and the second derivative operator, followed by hysteresis thresholding. Boudegga and coauthors [17] presented a new U-form deep learning architecture with convolution blocks for retinal vessel segmentation. Chavan and coauthors [18] used the K-means procedure to deal with the noise accompanying the recurring erosion operations needed to extract blood vessels. Sathananthavathi and coauthors [19] used the Encoder Enhanced Atrous (EEA) architecture of deep learning for blood vessel segmentation. Samuel and coauthors [20] applied a two-stage vessel extraction process, using a vessel- specific convolution block in the first stage and a skip chain convolution layer in the second. Atli and coauthors [21] used Sine-Net, with its upsampling and downsampling processes, to extract thick and thin blood vessels. Balasubramanian and coauthors [22] used mean orientation-based segmentation and applied a convolutional neural network (CNN) to extract blood vessels from segmented regions. Du and coauthors [23] used a Pyramid Scene Parsing (PSP) U-net-based segmentation algorithm for the same purpose. Lai and coauthors [24] used 4 models to identify the left/right eye. The first two are based on optic disc localization, while the third and fourth are based on the local binary pattern and fine-tuned ResNet-18, respectively. Tan and coauthors [25] proposed a technique which uses the central retinal vessel from the optic disc to identify the left/right eye.

## MATERIAL AND METHODS

This work proposes the two techniques below:

- i. Identifying the OD/OS using the DWT – The technique uses the DWT for optic disc (OD) region estimation so as to identify the OD/OS.
- ii. Extracting blood vessels using a clip limit estimation technique – The technique uses a contrast improvement algorithm in which the clip limit is estimated after an analysis, followed by segmentation using the thresholding method. Figure 1 represents a flow diagram of the proposed technique used for the identification of the left or right eye.

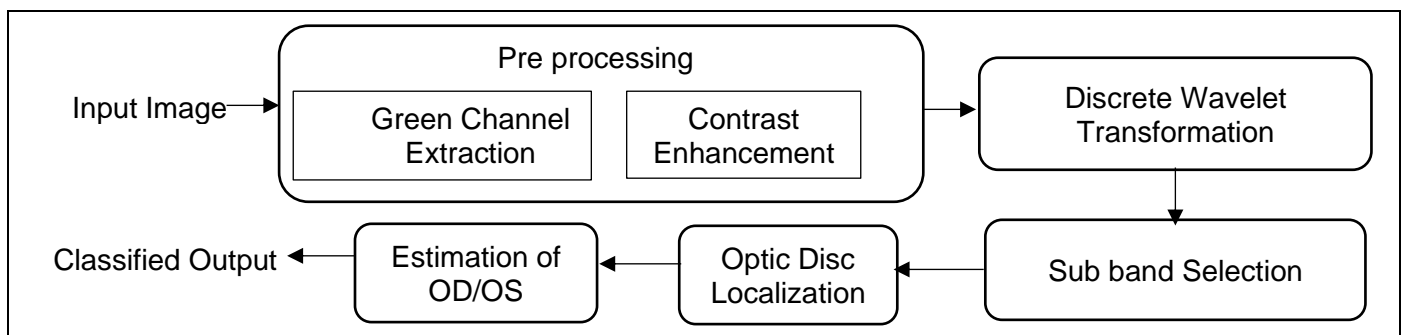


**Figure 1.** Flow diagram of the proposed technique for the identification of OD/OS

### Identification of OD/OS

The steps involved in OD/OS identification are described in the following sections.

#### Preprocessing

Preprocessing is an important step in digital image processing which helps in suppressing the unwanted distortions of an image and highlights the fine details of the image which is further used for analysis and processing. Here the preprocessing involves, green channel extraction and Contrast Enhancement

#### *Green channel extraction*

In general, retina images are color in nature. Retina images captured using fundus camera are highly sensitive to light. The blood vessels and the finer details present in the retina are clearly visible in green

channel when compared to red or blue channels. To be more accurate in extracting the blood vessels, green channel of the retina image is obtained.

### Contrast Enhancement

Contrast Limited Adaptive Histogram Equalization (CLAHE) divides the image into sub regions and histogram equalization is applied to each sub region for enhancement. CLAHE improves the contrast of the image which is used for further processing. After applying CLAHE the blood vessels of the retina and optic disc are clearly seen.

### Discrete Wavelet Transform

Localization of optic disc serves as a fundamental step in diagnosing different retinal abnormalities. By estimating the optic disc region it would be easy to identify OD/OS. In this work we used DWT to identify the optic disc region. DWT decomposes the image into sub bands, which results in less processing time. Rather than processing the entire image, a single band is taken for optic disc region estimation so that the processing time is also comparatively less. The image in the LH band is taken for the optic disc region estimation. Since the LH band contains the horizontal edges of the image, and the medical experts also uses horizontal view of the retina for detecting various defects and it is considered for the localization of optic disc.

### Sub band selection

DWT is applied on the contrast enhanced image which decomposes the image into four sub-bands namely LL, LH, HH, HL. Each of these sub bands contains various details of an image. The LL band contains the original image which is the lowest frequency band. The information in LL band is used for reproducing the original image. The LH sub band contains the horizontal features of the input image. HH sub band contains the vertical edges of the input image and last band HL contains the diagonal edges of the input image. Out of all the four sub bands, the LH band contains the most significant information like the brighter portion of the retina. Hence this band is used for further decomposition in identifying the OD/OS.

### Optic disc region estimation using Discrete Wavelet Transform (DWT)

The LH band is divided into two equal halves as 'm' region and 'n' region. The proposed algorithm traverses from the top left of 'm' region to the right bottom of middle portion 'v' thereby calculating the number of white pixels in the 'm' region of the image. This algorithm also traverses from the top left of the 'n' region to the right bottom of the 'n' region in the LH band thereby calculating the number of white pixels in the 'n' region of the image. The region which contains more number of white pixels are considered as the optic disc region. The number of white pixels in the 'm' region is compared with the 'n' region of the image. The results are also proved to be promising on applying this technique on the retina images. The region in the LH band is termed as  $x$ . The size of the  $x$  is computed. The mid value  $v$  of the region  $x$  is computed by dividing the region into equal halves as shown in Figure 2.

The mid value of the input image  $x$  is calculated using Equation (1)

$$v = x/2 \quad (1)$$

The number of pixels in the 'm' region is computed and stored in a variable say lcount. Similarly the number of white pixels in the 'n' region is computed and stored in a variable say rcount. The cumulative number of pixels are computed and stored accordingly. The cumulative sum of white pixels or 'm' region and 'n' region of the image in the LH band are calculated using Equation (2) and Equation (3)

$$m_c = \sum_{i=m}^v lcount + 1 \quad (2)$$

$$n_c = \sum_{j=v+1}^n rcount + 1 \quad (3)$$

This process is repeated until all the pixels are taken for evaluation. On counting the white pixels in the 'm' and 'n' region, the optic disc region is estimated. The region which has more number of white pixels is

considered to be the place where the optic disc is located. From this it is observed, that if the ‘m’ region of the image contains more number of white pixels then the eye belongs to the left side. If the ‘n’ region of the image contains more number of white pixels then the eye belongs to the right side. The steps applied in this process are described below.

No. of white pixels in m region →  $W_m$   
 No. of white pixels in n region →  $W_n$

if  $W_m > W_n$   
 Left else Right

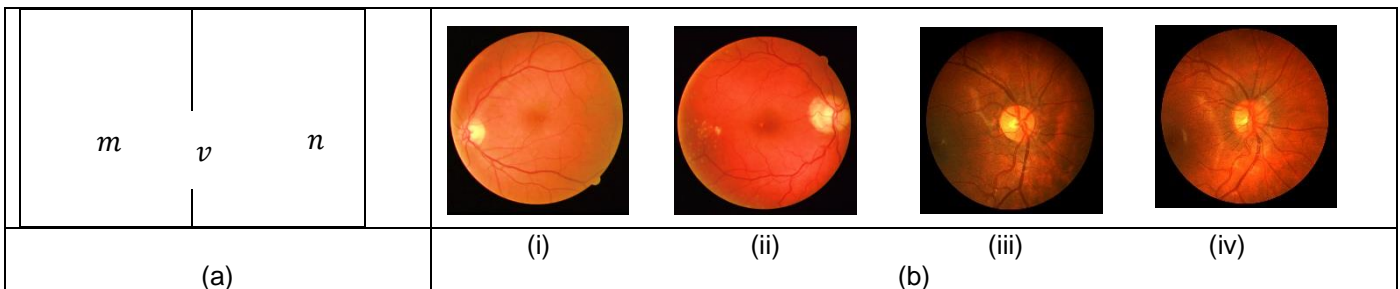


**Figure 2.** (a) Division of LH band (b) Sample retina images (i) The left eye, (ii) The right eye (iii) The left eye with optic disc in the middle (iv) The right eye with the optic disc in the middle

**Extraction of blood vessels**

Retinal blood vessels play a significant role in carrying oxygen to the brain, thus transmitting light to the retina to produce vision. They also depict bifurcations, internal crossovers, and diminishing endings. Such abnormalities in blood vessel extraction are indicative of ophthalmologic disease. In addition, cardiovascular and kidney diseases may be identified by analyzing the vessels. Consequently, the extraction of retinal blood vessels is invaluable in tracking disease in the human body. The presence of an unnecessary object like the optic disc, coupled with the noise and background, are key issues in such extraction. Figure 3 represents the proposed framework used to extract blood vessels.

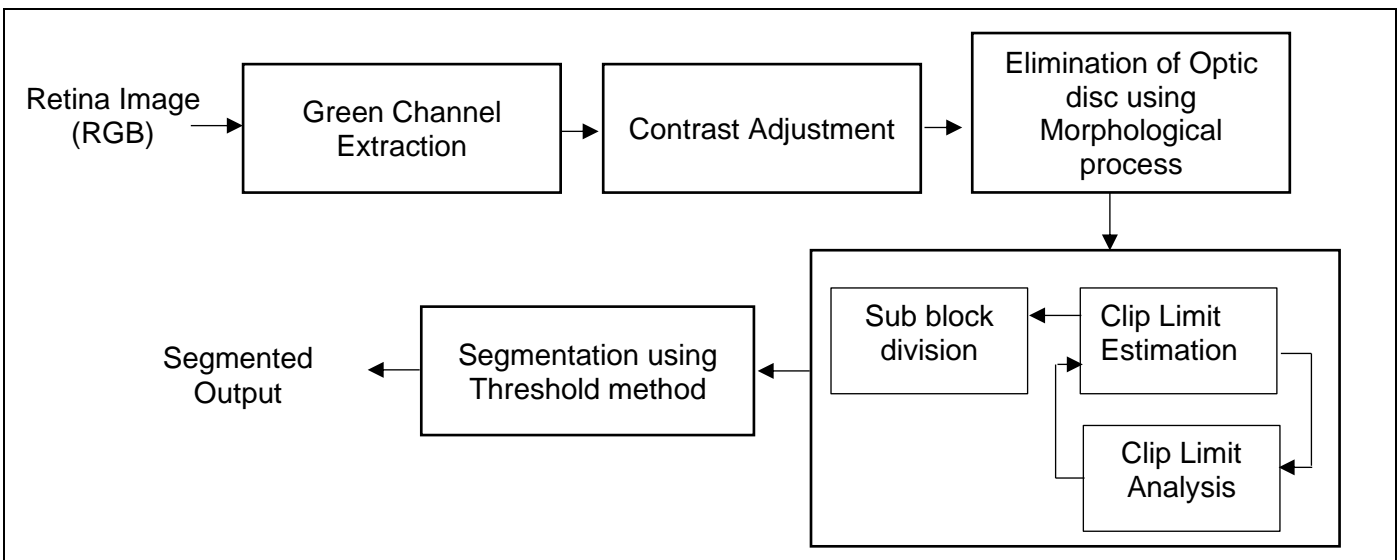


**Figure 3.** Proposed framework for the extraction of blood vessels

**Green channel extraction**

In the proposed framework, high-quality colored fundus images from different datasets are used for blood vessel extraction. Significant blood vessel features are clearly seen in the green channel of the image, rather than in the red and blue. Although only the green channel of the image is extracted for retinal vessels of the best quality, salient image features like sharpness, structure, characteristics and contrasts are retained. The image extracted from the green channel appears similar to a grayscale image.

## Contrast adjustment of the image

A high-contrast image looks brighter than the rest. Thin and thick retinal blood vessels are clearly visible when the contrast of the retinal image is adjusted.

## Elimination of the optic disc

The optic disc is the brightest portion of the retina, with the blood vessels originating here. In this work, the optic disc is removed from the retina to facilitate blood vessel extraction. The radius of the optic disc is estimated by applying the logical complement operator on the bright optic disc region of the retinal image to convert it into a dark region. The dark blood vessel regions are turned bright. The optic disc is circularly shaped, and the experimental analysis reveals that the radius is estimated to be around 8 to 10 pixels. A disc-shaped structuring element is considered for morphological processing, and an erosion operation is applied on the image so that the optic disc is completely eliminated.

## Clip Limit Estimation Technique for contrast improvement

There are two major challenges in blood vessel extraction in the retinal image.

(i) Firstly, the blood vessel width is not uniform and, secondly, it is difficult to segment tiny vessels from the background. The Contrast Limited Adaptive Histogram Equalization (CLAHE) is commonly used in medical image analysis to improve the visual quality of images. The contrast improvement technique is widely used for retinal image analysis, as is evident from the literature on the subject. The technique enhances retinal blood vessels such that further processing, in terms of blood vessel segmentation, is carried out easily. The Contrast Limited Adaptive Histogram Equalization (CLAHE) technique is a variant of the adaptive histogram equalization technique which, with its limited amplification, controls problems with noise amplification.

The CLAHE technique involves the following steps:

1. The input image is divided into 4 non-overlapping, equal-sized sub-regions.
2. A histogram is generated for each sub-region.
3. The clip limit is set and the total number of excess pixels identified.
4. The excess pixels are distributed to other bins.
5. Step 4 is repeated until all the excess pixels are redistributed.
6. The sub-regions are merged using the bilinear interpolation technique.

The Contrast Limited Adaptive Histogram Equalization (CLAHE) technique divides the complete image into equal-sized sub-regions/tiles. Tiles of different sizes may also be used and a histogram is generated for each. A small tile makes a narrow range of intensity values in the histogram a possibility. Further reductions in tile size complicate the process, with every chance of pixel loss occurring while the pixels are being connected together. With a bigger tile size, there is a possibility of obtaining a dynamic range of intensity values. In this work, the retinal image is divided into 4 equal-sized sub-regions. It is observed from the experimental analysis that dividing the retinal image, or any medical image, into 4 equal-sized sub-regions is most effective and produces the best results.

## Clip Limit Estimation

The clip limit value in the CLAHE ranges from 0 to 1, though it is generally set to 0.01 in numerous studies. Raising the clip limit enhances the quality of the image while simultaneously creating problems with noise amplification. This work is motivated to identify a suitable clip limit that maximizes image quality with tolerable noise amplification. To this end, therefore, we propose a Clip Limit Estimation technique for contrast improvement that may be used for any image processing application. Qualitative, quantitative, histogram distribution and statistical analyses are carried out to determine a suitable clip limit.

The following section describes the analyses in detail.

### Qualitative analysis

The visual quality of the image is considered for a qualitative analysis. A visual assessment is widely used in image processing to evaluate the performance of the algorithm, starting from 0.01 and increasing the clip limit value by 0.01. Once the clip limit value is estimated, image quality is further refined with an acceptable noise amplification level. A suitable clip limit is identified, beyond which the background non-ROI region and background pixels become bright enough to be highlighted. Table 1 shows the visual quality of the image for various clip limit values.

**Table 1.** Various clip limit values and their corresponding qualities

Clip limit Value	Visual Assessment
0.01	Good
0.02	Good
0.03	Very good
0.04	Fair
0.05	Poor

### Intensity distribution analysis

The distribution of pixels along the histogram bins is also considered for quality assessment in image enhancement. For quality images, it is essential that image pixels are distributed throughout the spectrum. The image will be either dark or bright when the pixel distribution is uneven. This fact has been considered in the analysis of the pixel distribution for various clip limits. Table 2 shows the pixel distribution range for various clip limit values.

**Table 2.** Range of pixel distribution for clip limit values

Clip limit Value	Range of pixel Distribution
0.01	1-238
0.02	1-247
0.03	1-252
0.04	1-256
0.05	1-256

When the clip limit value is 0.01, pixel distribution is limited to the gray-level range from 1 to 238 and seems uneven. Similarly, when the clip limit is 0.02, the pixel distribution seems to range from 0 to 247, though a uniform distribution cannot be ensured even at this point. As the clip limit is set to 0.03, the pixel distribution ranges from 0-252. The visual quality of the retinal image is appealing as well with the clip limit set to 0.03, rather than 0.01 and 0.02. With clip limits of 0.04 and 0.05, despite the seemingly even distribution, the background pixels are highlighted and might result in misclassification and reduced segmentation accuracy.

### Quantitative analysis

Further, a quantitative analysis is carried out by segmenting the contrast- improved image and counting the number of pixels in the segmented results. Parameters such as true positive (TP), false positive (FP), true negative (TN) and false negative (FN) are calculated by comparing the segmented results with ground truth images. An increase in the true positive and true negative rates corresponds with an increase in the clip limit value. The value of the true positive (blood vessels) is also greatly reduced. Table 3 shows the changes in the TP, FP, TN, and FN rates with respect to clip limit values.

**Table 3.** Clip limit values and corresponding values for quantitative parameters

Clip limit Value	Quantitative Parameters			
	TP	FP	TN	FN
0.01	11508	1142	300470	16840
0.02	21528	9872	291740	6820
<b>0.03</b>	<b>25606</b>	<b>30403</b>	<b>271209</b>	<b>2742</b>
0.04	6048	156595	145017	22300
0.05	6128	157252	144360	22220

There is a gradual increase in the TP rate for the clip limit values of 0.01, 0.02 and 0.03. There is a large difference in terms of values for the TP, FP, TN and FN parameters when the clip limit changes from 0.03 to 0.04, and so on. The increase in the false positive rate makes it clear that the background pixels are also identified as blood vessels.

### Statistical analysis

Statistical testing determines the relationship or quantitative decisions of the variables involved in the process. It is to be ensured that a uniform pixel distribution is carried out. A Q-Q plot may be used to analyze the pixel distribution. A Q-Q plot testing has been undertaken on the histogram to check the uniformity of the image pixel distribution for each clip limit. If the points of the Q-Q graph fall exactly in a straight line, it is recognized as normally distributed data. Figure 4 represents the Q-Q plot graph that depicts normal pixel distribution.

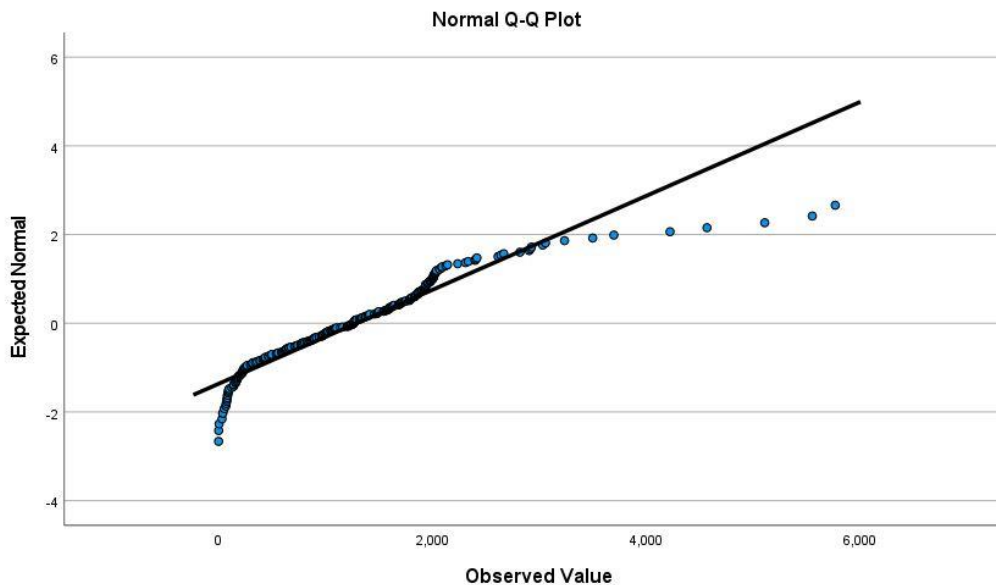


**Figure 4.** Q-Q plot for clip limit 0.03

This graph is generated for the contrast-enhanced retinal image with a clip limit of 0.03. In Q-Q plot, the 'expected normal' is denoted by the slope which represents the expected distribution of pixels for the enhanced images. The 'observed value' is denoted by the points (●) which represents the actual distribution of the pixels of an enhanced image. It is clear from Figure 4 that the actual value almost matches with the expected values in the Q-Q plot for clip limit 0.03, with most of the points lying in a straight line on the graph, showing that the data are uniformly distributed. Therefore, the clip limit for contrast enhancement may be set to 0.03, thus ensuring uniform pixel distribution.

### Clipping process

The clip limit ( $\gamma$ ) value in this work, which is determined using the proposed clip limit estimation technique, is considered for further processing. Pixels available beyond the clip limit value  $\gamma$ , which are termed excess pixels, are clipped and shifted to other bins using a uniform distribution strategy.

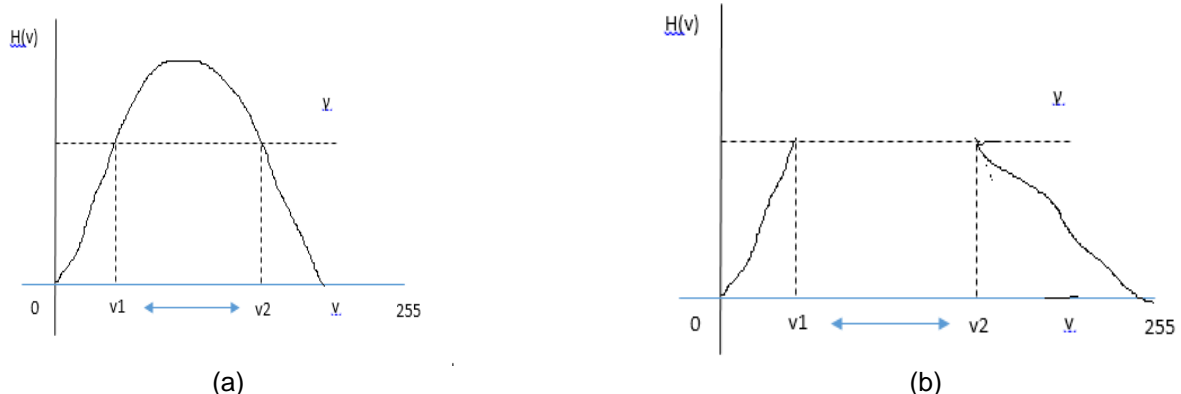


**Figure 5** a) Before clipping process b) Histogram after the clipping and distribution of excess pixels

The excess pixels clipped, which are denoted as 'm', are distributed to other bins uniformly until the pixels become null in a process. The excess pixel distribution makes the histogram equalized so that it improves the contrast of the image. Individual sub-regions are enhanced and neighboring sub-regions merged by applying the bilinear interpolation technique, which eliminates artificially created boundaries during the enhancement process. Bilinear interpolation is used to highlight the background pixels and eliminate pixel loss. Histogram before and after the clipping process is shown in Figure 5 (a) and (b).

### Blood vessel extraction using the thresholding technique

Thresholding is the simplest form of segmentation. With a visually good preprocessed image, the thresholding technique is most appropriate for the segmentation of the contrast-improved image. A single thresholding technique takes less computational time than the others. In this work, the retinal blood vessels are considered the region of interest (ROI). If the pixel intensity value is less than or greater than the specified threshold value, the pixel is identified either as a background pixel or a blood vessel, respectively.

$$g(x, y) = \begin{cases} 1, & \text{if } f(x, y) \geq T \\ 0, & \text{if } f(x, y) < T \end{cases} \quad (4)$$

Equation (4) gives the general form of the thresholding technique where  $g(x, y)$  is the output segmented image,  $f(x, y)$  the input image and  $T$  the threshold value. Figure 6 represents the segmented output obtained on applying the threshold technique.

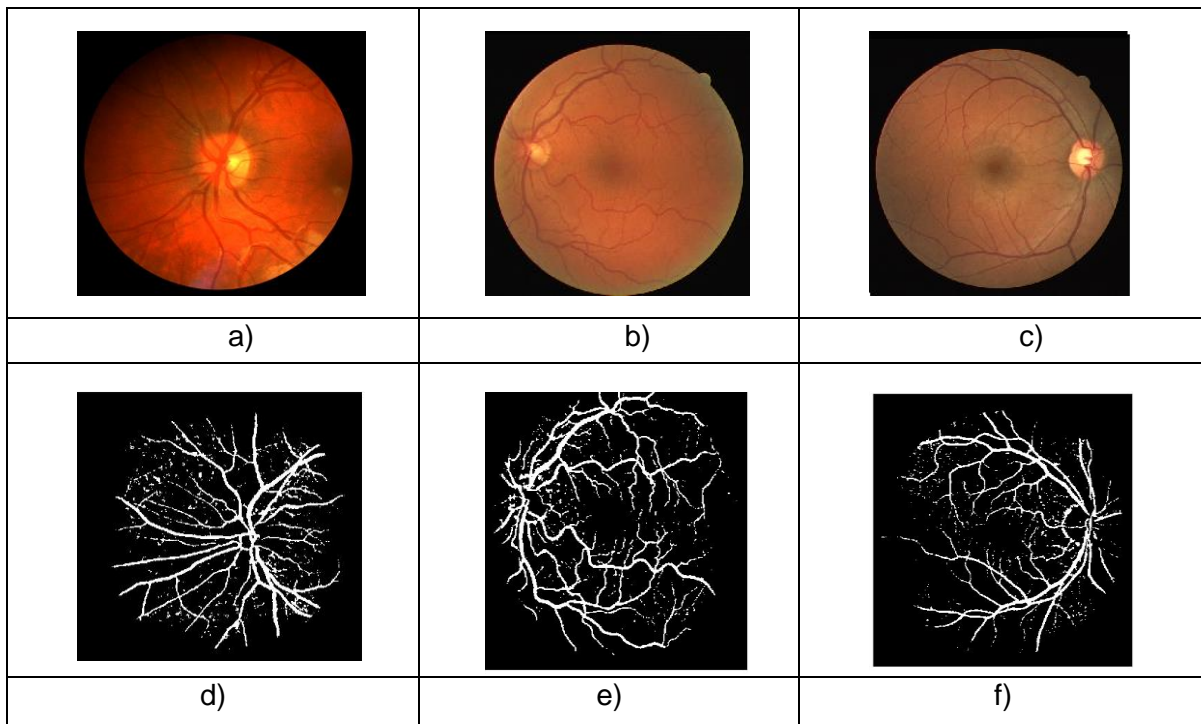


**Figure 6 (a → c)** Input retina images **(d → f)** The segmented results using the thresholding technique

### Experimental Results and Performance Analysis

The following experiments are carried out to evaluate the performance of the proposed technique:

- i. OD/OS identification using the proposed DWT-based technique
- ii. Clip limit estimation
- iii. Blood vessel segmentation using the proposed technique

### Datasets

For the experimental analysis, popular retinal datasets such as DRIVE, VAMPIRE, HRF, DIARET\_DB1 and STARE are used. The images stored in the database are captured using a high-quality fundus camera. The datasets are described in the following sections.

### DRIVE dataset

The DRIVE dataset is a retinal image repository collected from a diabetic retinopathy screening program. It comprises 40 images in two categories, training and testing. Of the 40 images, 33 show no signs of diabetic retinopathy (normal) and 7 have a mild form of it. The RGB images in the dataset, measuring 768 x 584 pixels, are in the TIF format.

### VAMPIRE dataset

The VAMPIRE dataset is a collection of 8 retinal images sized 3900 x 3072, 4 with healthy retinas and 4 with age-related macular degeneration. The images are grey and in the BMP format.

### HRF (High-Resolution Fundus) dataset

As the name implies, the HRF dataset is a collection of 45 high-resolution images of pixel size 3504 x 2236. Of the 45 RGB retinal images in the .JPG format, 15 show healthy retinas and another 15 diabetic retinopathy, while the other 15 are glaucoma-affected retinas.

### DIARET\_DB1 dataset

The DIARET\_DB1 dataset contains 89 images, of which 84 show mild diabetic retinopathy while 5 show none. The RGB images in the dataset, measuring 1500 x 1152 pixels, are in the .PNG format.

### STARE dataset

The STARE dataset contains 20 retinal RGB images, measuring 700 x 605 pixels, in the .PPM format.

## Performance metrics

The following performance metrics shown in Table 4 are used to evaluate the performance of the proposed algorithms:

1. Classification accuracy, which helps measure classification performance, and

$$\text{Classification Accuracy} = \frac{\text{No. of correctly classified images}}{\text{Total no. of images}} * 100$$

2. Accuracy, sensitivity, and specificity to analyze the performance of blood vessel segmentation. True Positive (TP), True Negative (TN), False Positive (FP), False Negative (FN) values are calculated by considering all segmented output pixels and comparing them with ground truth image pixels.

True Positive (TP) – Blood vessel pixels (ROI) correctly segmented as blood vessel pixels

False Positive (FP) – Background pixels (NROI) wrongly segmented as blood vessel pixels

True Negative (TN) – Background pixels (NROI) correctly segmented as background pixels (NROI)

False Negative (FN) – Blood vessel pixels (ROI) wrongly segmented as background pixels (NROI).

**Table 4.** Performance metrics.

Metric	Description	Formula
Accuracy	The ability of extracting the blood vessels (ROI) correctly	$\text{Accuracy} = \frac{TP + TN}{(TP + TN + FP + FN)}$
Sensitivity	The ability of extracting the blood vessels (ROI) thereby eliminating the background pixels (Non-ROI)	$\text{Sensitivity} = \frac{TP}{(TP + FN)}$
Specificity	The ability of extracting the background pixels (Non-ROI) and eliminating the blood vessels (ROI) pixels	$\text{Specificity} = \frac{TN}{(TN + FP)}$

## Experiment #1

### Performance of the proposed DWT-based technique for OD/OS identification

A DWT-based technique is applied on different dataset images for the identification of the OD/OS. Four datasets are taken for evaluation. Table 5 shows the performance of the proposed DWT-based technique for OD/OS eye identification.

**Table 5.** Performance of the proposed DWT-based technique for OD/OS identification for various datasets

Dataset	Total no. of images		Correctly Classified		Accuracy (%)
	Left	Right	Left	Right	
DRIVE	13	27	12	24	95.00
DIARET_DB1	46	41	41	41	94.30
VAMPIRE	4	4	3	4	87.50
HRF	21	24	21	23	97.70
<b>Average Accuracy</b>					<b>93.62</b>

The proposed algorithm correctly classifies the OD/OS in most cases. The HRF dataset with its high-resolution images offers the highest accuracy. Only a few images in the datasets are wrongly classified, the reasons being the

- (i) Unusual localization of the optic disc, owing to eyeball movement
- (ii) Angle from which the retinal image is captured
- (iii) Uneven illumination in capturing the image

Figure 7 represents an image (AMD1) from the VAMPIRE dataset, which is wrongly classified because of the unusual localization of the optic disc and uneven illumination.



**Figure 7.** Wrongly classified image (AMD1) from the VAMPIRE dataset.

### Experiment #2: Performance of the proposed clip limit estimation technique

In order to estimate the clip limit, analyses of a qualitative, intensity distribution, quantitative and statistical testing are carried out and an appropriate clip limit is estimated. The results of the analyses are shown in Tables 1-3 and Figure 4. The clip limit value of 0.03 is considered for contrast improvement in retinal images and for further processing.

### Experiment#3: Segmentation using simple thresholding

The retinal image is enhanced using clip limit estimation, followed by a simple thresholding technique which is applied on the image to extract blood vessels. The threshold value in this work is user-defined and set to 103. Table 6 shows the performance for the clip limit value of 0.03.

**Table 6.** Experimental results of the proposed work on testing images (Manual 1 and Manual 2) of the DRIVE dataset

INPUT IMAGE	Manual 1			Manual 2		
	ACCURACY (%)	SENSITIVITY (%)	SPECIFICITY (%)	ACCURACY (%)	SENSITIVITY (%)	SPECIFICITY (%)
01_test	96.25	73.31	98.50	96.50	75.20	98.54
02_test	96.17	67.06	99.49	96.54	69.15	99.61
03_test	95.17	65.56	98.45	95.92	71.67	98.29
04_test	95.52	53.69	99.76	95.95	56.35	99.76
05_test	95.72	60.14	99.40	96.99	69.47	99.42
06_test	95.58	59.73	99.44	96.02	62.53	99.46
07_test	95.47	58.60	99.18	96.78	70.12	98.84
08_test	95.54	63.36	98.57	96.44	74.00	98.04
09_test	96.01	65.60	98.70	96.14	66.46	98.75
10_test	95.94	58.48	99.30	96.80	65.70	99.2
11_test	95.73	60.88	99.15	96.51	66.44	99.24
12_test	96.22	70.33	98.66	96.76	75.24	98.64
13_test	95.26	57.11	99.39	95.06	55.91	99.47
14_test	96.32	72.13	98.45	96.78	77.05	98.37
15_test	96.38	67.19	98.63	95.94	63.54	98.55
16_test	95.91	61.58	99.32	96.79	67.47	99.52
17_test	95.71	69.11	98.16	96.48	77.01	98.03
18_test	96.32	70.20	98.57	96.51	68.46	99.35
19_test	97.07	73.73	99.18	95.99	64.45	99.47
20_test	96.59	68.91	98.78	95.84	60.98	99.4
MINIMUM	95.17	53.69	98.16	95.06	55.91	98.03
MAXIMUM	97.07	73.73	99.76	96.99	77.05	99.76
AVERAGE	95.94	64.83	98.95	96.33	67.86	98.99

The proposed work is tested on the DRIVE dataset images. The results shown in Table 6 are obtained by applying contrast improvement, using a clip limit of 0.03. The background pixels are correctly identified as such and thick retinal blood vessels correctly segmented. Table 7 represents the compiled retinal blood vessel segmentation results of the DRIVE, HRF, STARE, and DIARETDB1 datasets.

**Table 7.** Performance of the proposed technique for blood Vessel segmentation

Dataset	No. of Images	ACCURACY (%)	SENSITIVITY (%)	SPECIFICITY (%)
DRIVE		95.94	64.83	98.95
(MANUAL 1	20	96.33	67.86	98.99
MANUAL 2				
TRANING SET)	20	96.87	64.68	98.77
HRF	45	96.89	67.34	98.81
STARE	20	97.34	69.82	98.71
DIARETDB1	89	97.52	69.23	98.23

The results show enhanced accuracy for the DRIVE and HRF dataset images. Further, thick blood vessels and a few thin ones were extracted using the proposed method. The highest accuracy of 97% is obtained for test images of the DRIVE, STARE, and DIARETDB1 datasets, thus proving that the proposed method works well for retinal blood vessel extraction.

## Comparison with existing work

A lot of research has been carried out on retinal vessel segmentation, with a focus on different methods for retinal blood vessel extraction. Table 8 represents a comparative analysis of existing segmentation techniques with the proposed method.

**Table 8.** Comparative analysis of the proposed method with existing techniques

Technique	Dataset	ACCURACY (%)	SENSITIVITY (%)	SPECIFICITY (%)
Ozkava et al., 2018 [4]	DRIVE	95	85	98
Ganesan P et al.,2017 [6]	DRIVE	95	66	96
Roychowdhury et al., 2015 [22]	DRIVE, CHASEDB1	94	73	97
Mendonca et al., 2006 [23]	DRIVE, STARE	94	73	98
You et al. ,2011 [24]	DRIVE, STARE	94	74	97
<b>Proposed Method</b>	DRIVE, STARE, HRF, DIARETDB1	<b>97.52</b>	<b>69.23</b>	<b>98.23</b>

Ozkava and coauthors [4] and Ganesan and coauthors [6] used morphological operations for blood vessel segmentation. Roychowdhury and coauthors [22] used an iterative model for the same and obtained 94%. Mendonca and coauthors [23] used a morphological reconstruction technique for segmentation to produce 94% accuracy. The researchers behind [22] and [23] concluded that their techniques identify thick vessels. The proposed method produced better results in terms of accuracy than other work of its kind and, in addition, facilitated the extraction of most of the hair-like thick and thin blood vessel structures.

## DISCUSSION

This research has made two major contributions. The first contribution/work uses the DWT to identify the OD/OS. The technique divides the image into four sub-bands. Rather than process the entire image, a single sub-band is taken into consideration to reduce processing time. Here, the LH band with horizontal features of the image is taken. Given that processing the entire retinal image for optic disc region estimation takes time, only one sub-band is used for the OD/OS identification. The second contribution/work employs contrast improvement, through the use of clip limit estimation, to extract blood vessels. Imperfections in retinal medical images are greatly reduced by enhancing the image using an estimated clip limit value, say 0.03. The proposed method makes it possible to view the origins of blood vessels and blood vessel branches clearly. A qualitative analysis, an intensity distribution analysis, a quantitative analysis, and a statistical analysis are carried out to ensure uniform pixel distribution. Continuity nature, which is a characteristic of blood vessels, is maintained to enable accurate extraction using clip limit estimation, followed by the thresholding method. Performance analysis was carried out on the different datasets to demonstrate the working of the proposed method, with the performance measured in terms of accuracy, sensitivity, and specificity.

## CONCLUSION

Retina of human consists of 'n' number of blood vessels. There can be abnormalities in the blood vessels that can lead to different diseases. To identify the defects, the blood vessels and the optic disc has to be detected. The proposed framework works in better way in identification of OD/OS by locating the optic disc which produced optimum results in identification. The framework used contrast improvement using clip limit estimation and thresholding method is used for the extraction of blood vessels. The proposed framework produced a satisfying results both in identification of OD/OS and extraction of blood vessels. This clip limit estimation technique may be used in analyzing different types of medical images also.

## REFERENCES

1. Hou Y, Lin M, Qiu X, He M, Zhang Y, Guo F. Effect of type-2 diabetes mellitus in retinopathy patients on MDA, SOD activity and its correlation with hba1c. *Braz Arch Biol Technol.* 2021;64. doi:10.1590/1678-4324-2021200075
2. 2.2 billion people globally suffer from eye conditions, visual impairment: Who. *News. India Today.* Oct 9, 2019. Available from: <https://www.indiatoday.in/education-today/latest-studies/story/two-billion-people-eye-conditions-visual-impairment-who-report-1607486-2019-10-09>. Accessed: 2022 Aug 31

3. Mohideen DF, Raj JS, Raj RS. Regression imputation and optimized Gaussian naïve Bayes algorithm for an enhanced diabetes mellitus prediction model. *Braz Arch Biol Technol.* 2021;64. doi:10.1590/1678-4324-2021210181
4. Ozkava U, Ozturk S, Akdemir B, Sevfi L. An efficient retinal blood vessel segmentation using morphological operations. 2018 2nd International Symposium on Multidisciplinary Studies and Innovative Technologies (ISMSIT). 2018; doi:10.1109/ismsit.2018.8567239
5. Aswini S, Suresh A, Priya S, Santhosh Krishna BV. Retinal vessel segmentation using morphological top hat approach on diabetic retinopathy images. 2018 Fourth International Conference on Advances in Electrical, Electronics, Information, Communication and Bio-Informatics (AEEICB). 2018; doi:10.1109/aeecib.2018.8480970
6. Ganesan P, Sathish BS. Automatic detection of optic disc and blood vessel in retinal images using morphological operations and Ipachi model. *Res J Pharm Technol.* 2017;10(8):2602. doi:10.5958/0974-360x.2017.00461.9
7. Dash J, Bhoi N. Detection of retinal blood vessels from ophthalmoscope images using morphological approach. *ELCVIA Electronic Letters on Computer Vision and Image Analysis.* 2017;16(1):1. doi:10.5565/rev/elcvia.913
8. Ramos-Soto O, Rodríguez-Esparza E, Balderas-Mata SE, Oliva D, Hassanien AE, Meleppat RK, et al. An efficient retinal blood vessel segmentation in eye fundus images by using optimized top-hat and homomorphic filtering. *Comput Methods Programs Biomed.* 2021;201:105949. doi:10.1016/j.cmpb.2021.105949
9. Xue L-Y, Lin J-W, Cao X-R, Yu L. Retinal blood vessel segmentation using saliency detection model and region optimization. *J Algorithm Comput Technol.* 2017;12(1):3–12. doi:10.1177/1748301817725315
10. Lestari T, Luthfi A. Retinal blood vessel segmentation using Gaussian filter. *J Phys Conf Ser.* 2019;1376(1):012023. doi:10.1088/1742-6596/1376/1/012023
11. Rahmani AI, Akbari H, Esmaili SS. Retinal blood vessel segmentation using gabor filter and morphological reconstruction. *Signal Processing and Renewable Energy.* 2020 Mar 1;4(1):77–88.
12. Nugroho HA, Lestari T, Aras RA, Ardiyanto I. Segmentation of retinal blood vessels using Gabor wavelet and morphological reconstruction. 2017 3rd International Conference on Science in Information Technology (ICSITech). 2017;513–6. doi:10.1109/icsitech.2017.8257166
13. Yavuz Z, Kose C. Retinal blood vessel segmentation using Gabor filter and top-hat transform. 2011 IEEE 19th Signal Processing and Communications Applications Conference (SIU). 2011;546–9. doi:10.1109/siu.2011.5929708
14. Sathya N, Karuppasamy K, Suresh P. Contourlet transform and morphological reconstruction based retinal blood vessel segmentation. *Int J Biomed Eng Technol.* 2017;25(2/3/4):105–19. doi:10.1504/ijbet.2017.087710
15. Halder A, Sarkar A, Ghose S. Adaptive Histogram Equalization and opening operation-based blood vessel extraction. *Soft Computing in Data Analytics.* 2018;557–64. doi:10.1007/978-981-13-0514-6\_54
16. Dash S, Senapati MR, Sahu PK, Chowdary PS. Illumination normalized based technique for retinal blood vessel segmentation. *Int J Imaging Syst Technol* 2020;31(1):351–63. doi:10.1002/ima.22461
17. Boudegga H, Elloumi Y, Akil M, Hedi Bedoui M, Kachouri R, Abdallah AB. Fast and efficient retinal blood vessel segmentation method based on Deep Learning Network. *Comput Med Imaging Graph.* 2021;90:101902. doi:10.1016/j.compmedimag.2021.101902
18. Chavan A, Mago G, Balaji J, Lakshminarayanan V. A new method for quantification of retinal blood vessel characteristics. *Ophthalmic Technologies XXXI.* 2021;113–20. doi:10.1117/12.2576984
19. Sathananthavathi, Vallikutti, and Ganesan Indumathi. BAT algorithm inspired retinal blood vessel segmentation. *IET Image Processing* 12.11 (2018): 2075-83.
20. Samuel PM, Veeramalai T. VSSC net: Vessel specific skip chain Convolutional Network for blood vessel segmentation. *Compu Methods Programs Biomed.* 2021 Jan 1;198:105769. doi:10.1016/j.cmpb.2020.105769
21. Atli İ, Gedik OS. Sine-net: A fully convolutional deep learning architecture for retinal blood vessel segmentation. *Eng Sci Technol Int J.* 2021 Apr 1;24(2):271–83. doi:10.1016/j.jestch.2020.07.008
22. Roychowdhury, Sohini, Dara D. Koozekanani, and Keshab K. Parhi. Iterative vessel segmentation of fundus images. *IEEE Trans Biomed Eng* 62.7 (2015): 1738-49.
23. Mendonca AM, Aurelio Campilho. Segmentation of retinal blood vessels by combining the detection of centerlines and morphological reconstruction. *IEEE Trans Med Imaging* 25.9 (2006): 1200-13. Lai X, Li X, Qian R, Ding D, Wu J, Xu J. Four models for automatic recognition of left and right eye in fundus images. *MultiMedia Modeling.* 2018;507–17. doi:10.1007/978-3-030-05710-7\_42
24. You X, Peng Q, Yuan Y, Cheung Y. Segmentation of retinal blood vessels using the radial projection and semi-supervised approach. *Pattern recognition.* 2011; 44(10):2314-24.



© 2023 by the authors. Submitted for possible open access publication under the terms and conditions of the Creative Commons Attribution (CC BY NC) license (<https://creativecommons.org/licenses/by-nc/4.0/>).